



HAL
open science

Characterization of the texture of large hailstones

Maurine Montagnat, Mathieu Bourcier, Armelle Philip, Paul D Bons,
Catherine C Bauer, Paul Deconinck, Pierre Hereil

► **To cite this version:**

Maurine Montagnat, Mathieu Bourcier, Armelle Philip, Paul D Bons, Catherine C Bauer, et al..
Characterization of the texture of large hailstones. 2020. hal-02942822

HAL Id: hal-02942822

<https://hal.science/hal-02942822>

Preprint submitted on 18 Sep 2020

HAL is a multi-disciplinary open access archive for the deposit and dissemination of scientific research documents, whether they are published or not. The documents may come from teaching and research institutions in France or abroad, or from public or private research centers.

L'archive ouverte pluridisciplinaire **HAL**, est destinée au dépôt et à la diffusion de documents scientifiques de niveau recherche, publiés ou non, émanant des établissements d'enseignement et de recherche français ou étrangers, des laboratoires publics ou privés.

Characterization of the texture of large hailstones

Maurine Montagnat^{1,2}, Mathieu Bourcier¹, Armelle Philip¹, Paul D. Bons³, Catherine C. Bauer³, Paul Deconinck⁴, and Pierre Hereil⁴

¹Univ. Grenoble Alpes, CNRS, IRD, G-INP, IGE, F-38041 Grenoble, France

²Univ. Grenoble Alpes, Univ. Toulouse, Météo-France, CNRS, CNRM, Centre d'Études de la Neige, 38000 Grenoble, France.

³Departement of Geosciences, Eberhard Karls University Tübingen, Germany

⁴Thiot ingénierie, Puybrun, France

Correspondence: Maurine Montagnat (maurine.montagnat@univ-grenoble-alpes.fr)

Abstract. Hailstone structures have been studied for over a century, but so far mainly by manual optical means. This paper presents new texture and microstructure data (i.e. crystal lattice orientations, grain sizes and shapes) measured with an Automatic Ice Texture Analyzer (AITA) which gives access to high spatial and angular resolutions. The hailstones show two main characteristics; (i) they are structured with several concentric layers composed of alternating fine equi-axed grains and coarse elongated and radially oriented grains, (ii) they show two texture types with **c**-axes oriented either parallel or perpendicular to the radial direction. Such textures are compared with the ones observed in lake S1 and S2 ices, respectively. The S1 texture type (with **c**-axes parallel to the columnar crystals that grew in the radial direction) may result from epitaxial growth from a polycrystalline embryo, while S2 texture (**c**-axes in the plan perpendicular to the column direction) may result from the growth from an embryo made of large crystals with only one or few crystallographic orientations. Owing to these high resolution measurements of both microstructure and texture, we are able to come back to a long-term discussion concerning the growth mechanisms of large hailstones and clarify the main processes at play.

Copyright statement. TEXT

1 Introduction

Hail fall during thunderstorms can create severe damage and losses to agriculture, car holders and real estate. In terms of insured losses, the two hailstorms in Germany on 27-28 July 2013 were the costliest natural disasters worldwide in that year (Kunz and Kugel, 2015; Puskeiler et al., 2016). Aircraft are also strongly impacted by hailstones when passing through hailstone regions and clouds, potentially causing dramatic accidents.

Interest in studying hailstone microstructures is not new (Crammer, 1903) and was first motivated by the understanding of hailstone formation in clouds, based, for example, on isotopic studies associated with direct microstructural observations (Schuma, 1938; List, 1960; Knight and Knight, 1968; Jouzel et al., 1975; Macklin et al., 1976; Macklin, 1977). More recently, a large range of studies focused on understanding and modeling of the impact of hailstones on structures (see for example

Kim and Keune (2007); Anghileri et al. (2005)). In most of these studies, modeling approaches are validated with laboratory experiments in which hailstones are replicated by artificial ice samples, sometimes spherical, with microstructures that are most of the time far from realistic (Guégan et al., 2011; Combescure et al., 2011; Pernas-Sánchez et al., 2015).

25 Grain size and texture are known to influence the mechanical behavior of ice, in particular in the static brittle regime (see Schulson and Duval (2009) for a review). Impact of hailstones occurs in a dynamical regime (at strain rates higher than several s^{-1}) for which few studies have considered the effect of grain sizes and texture (here used to denote the distribution of crystallographic orientations). For most materials, it is assumed that porosity (density, shape and size distribution of pores) is mainly controlling fracture propagation during dynamic behavior (Forquin and Erzar, 2010). However, very few studies have
30 considered the effect of microstructure and texture under such conditions. This may be due to the lack of accurate data and the difficulty to design hail-like microstructures and textures.

Hailstone microstructure results from a complex formation history in cumulonimbus clouds, where atmospheric conditions induce several vertical movements in the cloud column. Hailstones are subjected to strong updraughts and downdraughts under conditions that can be constrained indirectly by measuring the isotopic signatures in the different ice layers forming the
35 hailstone (Macklin et al., 1976).

Hailstone growth results from the rapid freezing of supercooled water (Macklin, 1977). Depending on the temperature in the cloud at the time of the formation, only one part of the supercooled drops freezes instantaneously. Therefore, hailstone growth results into irregular microstructures, due to a balance between accretion rate, heat transfer, and the strong impact of temperature conditions, water content, and falling velocity. Such a complicated process results in layered microstructures as
40 illustrated in (Macklin et al., 1970; Jouzel et al., 1975; Knight and Knight, 2005).

Large hailstones are characterized by close to spherical or ovoid shapes, with alternating layers of “white” and “dark” ice. The difference between these layers is directly related to porosity and grain size. White (opaque) ice layers consist of very small grains that are surrounded by tiny air bubbles, and are supposed to grow under close to “dry” conditions, near the wet growth limit. Transparent layers (that appear “dark” in comparison to white layers) are supposed to form under “wet” conditions
45 during which a liquid layer remains in contact with the ice surface over longer periods (Macklin, 1977). In the transparent layers, grains are generally larger and the ice is relatively clear as air has time to escape during slow formation. Macklin (1977) was able to estimate the temperature of formation of large hailstones from careful evaluation of the isotopic content of the different layers associated with microstructure observations. While bubbly spherical embryos with small grains were shown to form at temperature close to -30°C , so-called frozen drop embryos would form at temperature between -10 to -15°C . In both
50 cases, the surrounding layers were shown to form in a temperature range of -17 to -30°C , corresponding to a height interval of 2 km in the atmosphere. At the same time, the author was able to estimate a liquid content of 4 to 5 g m^{-3} at the time of formation.

Some large air bubbles can be trapped and are frequently observed to be elongated in the direction of crystal growth. Knight and Knight (2005) refer to it as “icicle” type growth, with elongated growth in the direction of the temperature gradient, very similar
55 to what is observed in ice stalactites (Lliboutry, 1964; Montagnat et al., 2010). This type of microstructure is also similar to that observed in so-called “syntaxial” mineral veins, where the crystals grow side by side into a crack (Bons et al., 2012). As already

noticed by Macklin (1977), subsequent recrystallization can also occur after hailstones formation, especially when reaching higher temperatures on the ground. Knight and Knight (1968) made use of crystallographic *c*-axis orientations evaluated at low resolution by surface etching (Knight, 1966) to test the hypothesis of a "spongy" growth of hailstones. Hailstones are supposed to grow "spongy" when liquid water is trapped during the growth process and then freezes during the descent. Large columnar grains of outer shells were found to have their *c*-axes oriented radially, in the growth direction. From this observation Knight and Knight (1968) disproved the hypothesis of a spongy growth for the large hailstones they studied. Nevertheless, the *c*-axis orientation measurements were limited to one orientation per grain, and only to grains large enough to be evaluated by the etching method. They could not, therefore, evaluate the small grain shells, and the inner cores, where nucleation-determined orientations may be initiated.

In this study, we present the first high resolution microstructure and texture measurements on large hailstones (a few centimeters in diameters) that were gathered from the town of Tübingen in southwest Germany, during a violent storm of July 28th, 2013 (Kunz and Kugel, 2015; Puskeiler et al., 2016) and in the south west of France on August 31th, 2015. Our data can provide insights for the design of ice-growing techniques to better mimic natural hailstones, and could also offer complementary constraints for modeling-based approaches to simulate and predict hailstones formation and impact.

2 Characterization of hailstone textures

2.1 Hailstone collection

Hailstones from Germany were collected about a quarter of an hour after the storm that took place in the southwest German town of Tübingen, on July 28th, 2013. They were piled up on the street and balcony, while the temperature had dropped to about 20°C. They were subsequently stored at approximately -18°C until three of them (samples G1-3) were analyzed.

The French hailstones were collected by volunteers from ANELFA association (<http://www.anelfa.asso.fr/>), in the south west of France on August 31th, 2015. They were put in silicon oil, and kept at -28°C before being send to IGE were they were stored at -10°C until four of them were analyzed (samples F1-4). One of these large hailstones is illustrated in figure 1.

2.2 Method

Hailstone is composed of ice Ih which is a crystalline material with a hexagonal crystallographic structure. Owing to its birefringence, it is possible to define the orientation of the *c*-axis - also called the optical axis - under crossed polarizers. This *c*-axis is perpendicular to the basal plan of the hexagonal structure.

Thin sections of ice samples are shaved down to a thickness of about 300 μm with a microtome. This thickness is a necessary compromise to limit the effect of grain boundaries, and to keep a sufficient thickness for accurate automatic *c*-axis evaluation using the Automatic Ice Texture Analyzer (AITA) (Wilson et al., 2003). AITA determines the *c*-axis orientation for every pixels of the thin section at a resolution adjustable between 5 to 50 μm . In this work, the resolution was set to 10 μm as a necessary compromise between the size of the data files and the minimum measurable grain size (which is also constrained by

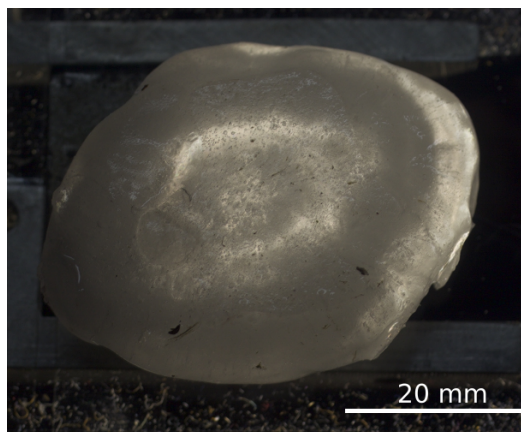


Figure 1. Flat hailstone from the South West of France (F1) observed under polarized light.

the thickness limit). The angular resolution is about 3° (Peternell et al., 2011). The AITA technique is therefore far superior to manual analysis, where only about one to 10 measurements per grain can reasonably be done, in large grains and with an angular resolution no better than 5 to 10° , strongly depending on the operator. The quality of the automatic determination of the **c**-axis orientation is estimated by AITA through a quality factor (QF) described in (Peternell et al., 2011). In agreement with the previous cited work, we use a QF threshold of 70 or 75 to remove the low quality measurements before further data treatment. By doing so, pixels from grain boundaries and bubbles are automatically removed.

All results obtained with the AITA are analyzed with an in-house python script (<https://github.com/ThomasChauve/aita>). This script draws map of the thin section, using a **c**-axis orientation based color lookup table (shown as inset in the figures). It also provides a pole figure of the **c**-axis orientations which corresponds to a lower-hemisphere, equal-area stereographic projection of the **c**-axis orientations (Fig. 2). To achieve a statistical representation, 10 000 randomly chosen pixels (all above the QF threshold) are displayed with the colour representing the density. Blue dots show orientations represented by only one pixel in the selection. Pole figures are shown in the (x,y) plan that corresponds to the thin section plan. The (Oz) axis is perpendicular to the thin section and to the figures, otherwise mentioned.

Thin sections are a 2D sample of a 3D object. In order to test the representativeness of the thin-section based data, two perpendicular sections of the same hailstone were analyzed. The orientation maps and pole figures (Fig. 3) of these two thin sections show that microstructures and textures are quite similar for both. This confirms, at least qualitatively, the concentric nature of the texture and microstructure. Most of the studied hailstones consist of quasi-ellipsoidal layers. In order to individualise the layers, we used elliptical masks (see Fig. 5 and 6).

Opaque or cloudy layers already show that the hailstones are porous (see for instance Fig.1). White pixels in the orientation maps further qualitatively indicate porosity (Fig. 2, and 3). However, X-ray microcomputed tomography (microCT) can be used to better reveal and quantify the porosity. We present a preliminary study made on a sample of dimensions $40 \times 20 \times 20 \text{ mm}^3$

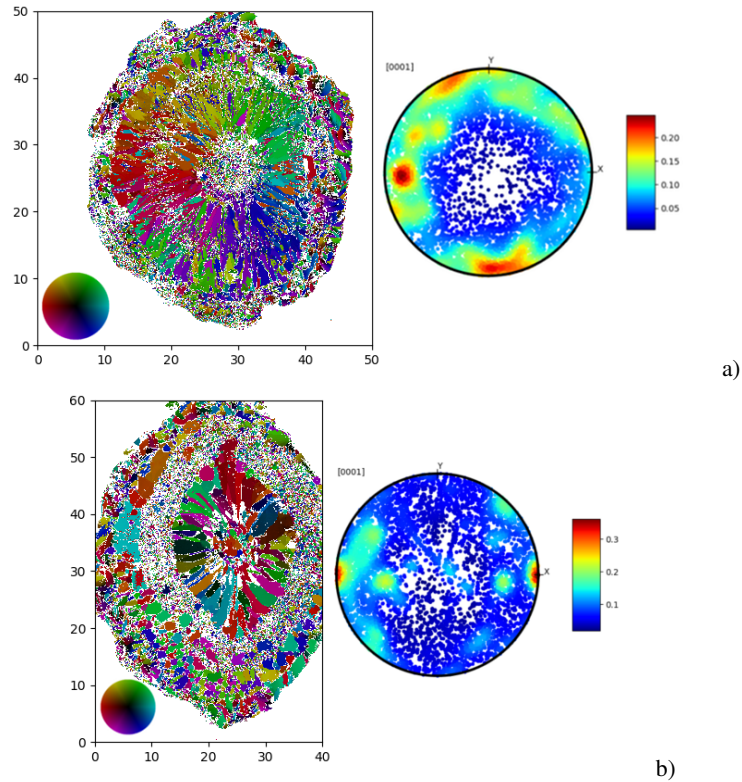


Figure 2. Illustration of AITA data obtained from German hailstone G1 (a) and French hailstone F1 (b). For each hailstone: Left: orientation color-coded image obtained after a filtering with QF set to 75. White areas are excluded for further analyses. The orientation color-code is given by the color wheel on the bottom left of the images (lower-hemisphere, equal area stereographic projection). Scale is mm. Different layers are identified and separated by dotted lines for clarity. Right: c-axis orientations plotted on a pole figure. The color-code corresponds to the density of pixels. The (x,y) plan is the plan of the thin section.

110 extracted from the French hailstone F2 (see Appendix). The sample was scanned with the Easytom XL nano tomograph from
 RX Solutions of the CMTC platform from Grenoble-INP (Fig. 4). The samples were maintained at -10°C in a cold cell during
 the acquisition (Burr et al., 2018). Two data acquisitions were done. One covering the whole sample volume with a (cubic)
 voxel size of $5\ \mu\text{m}$, and another one covering a smaller volume with a voxel size of $2\ \mu\text{m}$. The reconstruction of the 3D images
 from grayscale density images is facilitated by the high contrast between air and ice, which ensures an easy thresholding of the
 115 3D binary images. Figure 4 shows a 3D view of the reconstructed images for the two acquisitions. Some pores smaller than the
 voxel size cannot be resolved which may lead to errors in the segmentation and porosity estimation.

Since a full statistical evaluation of the porosity of hailstones is beyond the scope of the paper, we only provide the preliminary
 porosity data as an illustration. The porosity is estimated to be about 1.5% in volume fraction in the larger studied volume
 and about 2.2% in the smaller one. In this last volume, two very large pores account for 26.5% of the total porosity, each one

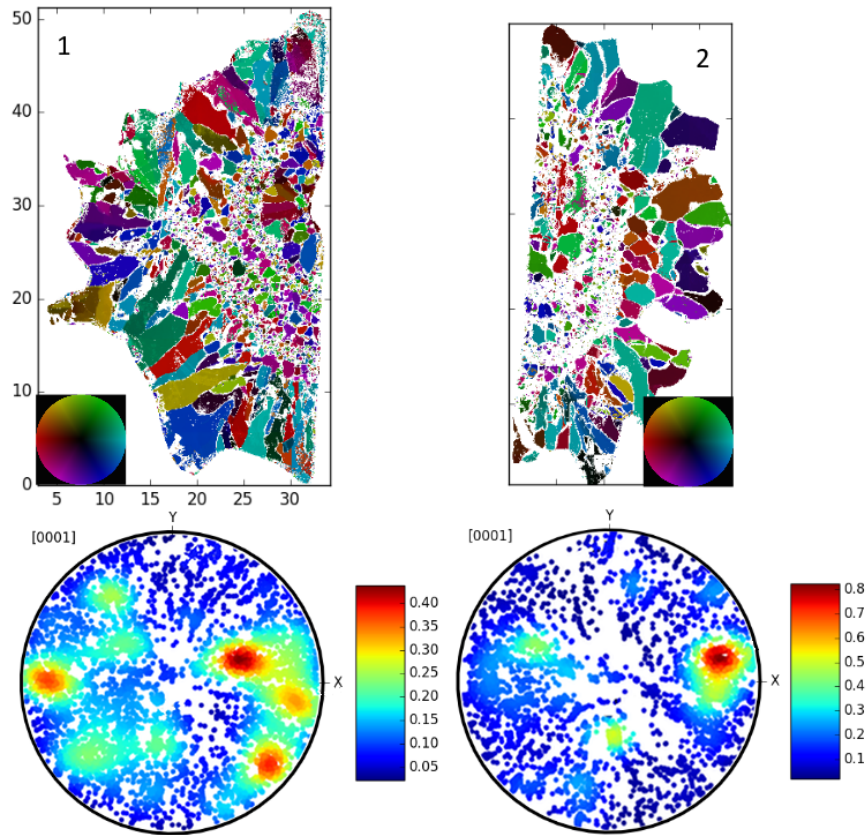


Figure 3. Microstructures and pole figures of two perpendicular thin sections French hailstone F2.

120 having a volume of about 0.1 mm^3 . Porosity appears very heterogeneously distributed within the different layers with small pores observed even in the transparent layers.

2.3 Observations and analyses

125 Seven large hailstones of diameter between 3.5 and 5 centimeters were studied, four from the South West of France storm (samples F1-4) and three from the German storm (samples G1-3). No clear distinction in the microstructures and textures could be made related to the geographic location of the presented hailstones. However, we have noticed two remarkable differences between the textures of the hailstones studied, on which we will focus in the following. This will be supported visually by detailed characterizations of two representative hailstones. Observations done on the other hailstones can be found in the appendix.

130 Hailstone F1 has a flat ellipsoid shape with a large axis of about 5.2 cm, a small axis of about 4 cm and a thickness of about 1.5

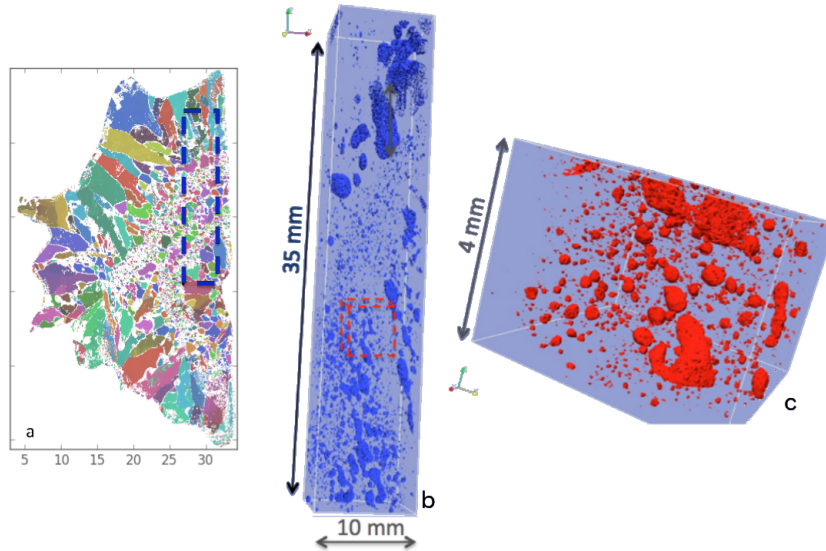


Figure 4. Visualization of the 3D porosity in one part of French hailstone F2 (a) with a resolution of $5 \mu\text{m}$ (b) and with a resolution of $2 \mu\text{m}$ (c). Various pore sizes are observed and seem to be distributed within the different layers.

cm (Fig. 1). The AITA analysis (Fig. 2) shows a concentric zonation with variations in grain size and shape. The pole figure of the entire hailstone shows a girdle-type texture, with most *c*-axes rather oriented in the plan of the thin section.

Fig. 5 represents four individual concentric parts that were isolated from the F1 hailstone microstructure, and their corresponding pole figures. The core of the hailstone is composed of a large grain surrounded by several smaller grains. It is important to
 135 note that the blue and red colors of the grains correspond to almost the same orientation but with opposite azimuth (see color wheel in Fig. 5). The core of hailstone F1 is therefore composed of several grains with almost identical *c*-axis orientations.

The first noticeable layer is composed of large grains elongated in the radial direction, which is the assumed growth direction (Knight and Knight, 2005). A close look at the intersection between the core and this layer in Fig. 2 reveals that this layer departed from smaller grains separated from the large grains by a porous area. In this layer, the texture is anisotropic, with a
 140 preferential orientation of *c*-axes in a girdle perpendicular to the plan of the thin section. The analysis of several individual grain orientations indicates that most of them have their *c*-axis oriented perpendicular to their growth direction (or their long axis), as denoted by the black arrows in Fig. 5.

The second layer is a fine-grained layer that corresponds to the opaque, porous layer in Fig. 1. This layer also has a girdle type *c*-axis distribution, with *c*-axes preferentially aligned close to the plan of the thin section. The slight misalignment could be
 145 due to the fact that the thin section was not cut in the exact center of the hailstone. The large number of small grains, many of them too small to be oriented, prevent from deciphering the orientation of the *c*-axes relative to the growth direction. The last layer is composed of large, more equiaxed grains, also characterized by a girdle-type *c*-axis distribution. In this layer, some of the large grains have their *c*-axes oriented in the growth direction, and some are oriented perpendicular to this direction. No

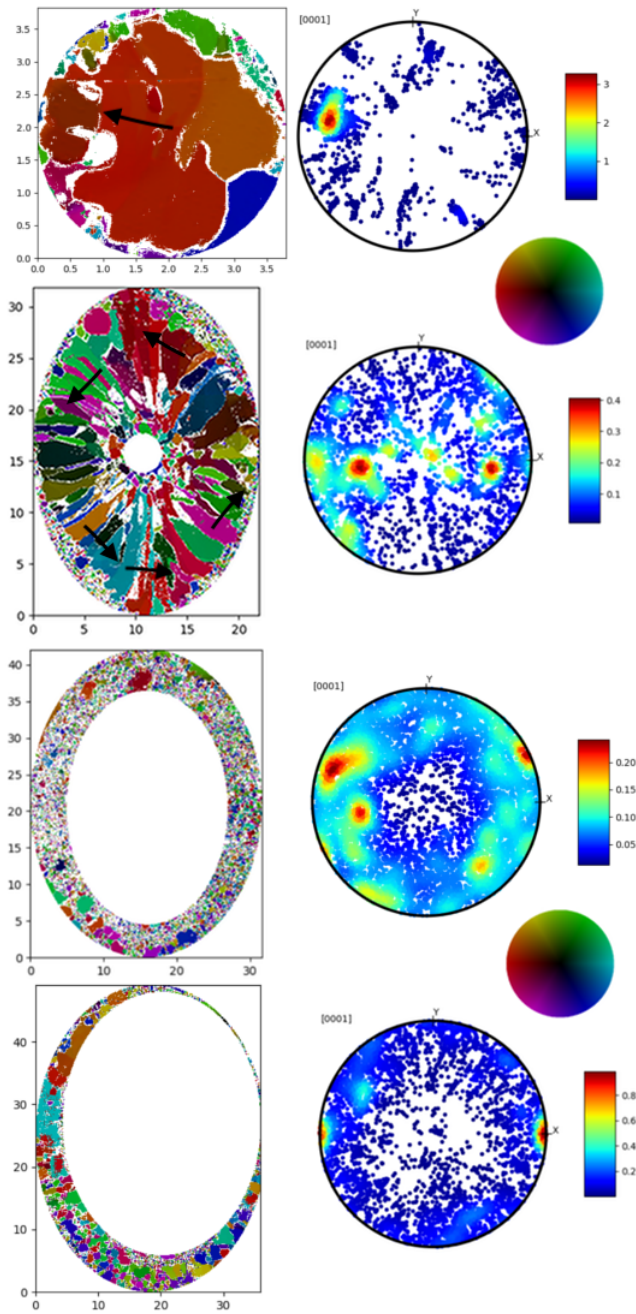


Figure 5. Extracted microstructures of the different observed layers in the French hailstone F1 with the corresponding pole figures. Core layer (top) to external layer (bottom). Black arrows sketch the orientation of the c -axes of a few selected c -axes to help with the analyses. The scale of the orientation color-coded map is in millimeter. The color code is provided by the color wheel.

clear trend can be extracted owing to the too limited number of grains in the layer.

150 The second hailstone used as an illustration is the German hailstone G1 (Fig. 2). One core and two individual layers could be clearly distinguished (Fig. 6). The last layer, being too complex, will not be commented here. The core is composed of many small equiaxed grains (about a hundred μm diameter). Both the first and second layers are composed of radially aligned elongated grains, but grains are smaller in the second layer. All three parts (core and layers) show a distribution of **c**-axes characterized by a girdle in the plan of the thin section. The colors in the microstructure images of the two external layers show
155 a remarkable match with the color distribution of the color wheel, which highlights the radial orientations of the **c**-axes.

3 Discussion

All hailstones studied here have in common that they are composed of concentric layers with different grain size, morphology and texture. Our high resolution measurements of **c**-axis orientations and microstructures revealed two specific textures. The
160 first type is represented by the F1 hailstone (Fig. 5 and Fig. A3 in the Appendix for hailstone F4). It includes samples composed of a nearly single-crystalline core, surrounded by a layer with large elongated grains with their **c**-axes oriented tangentially, perpendicular to the temperature gradient direction. These specific crystalline orientations and morphology are comparable to the so-called S2 lake ice (Michel and Ramseier, 1971) that would signify slow growth along the thermal gradient directions with little perturbations. **c**-axis orientations would, similarly to S2 ice, result from a selective growth process, also observed in
165 icicles extracted from frozen ice falls (Montagnat et al., 2010). Layers similar to the second layer of hailstone F1 are commonly observed in the hailstones studied. It is composed of fine grains with **c**-axes oriented with a relative isotropy in the thin section plan. A closer look at a few individual grains shows that both radial and tangential orientations are present (not shown here). Based on the grain size observation, we may assume that this layer is the result of the rapid frost on the hailstone surface of supercooled droplets present in the cloud. Our texture observations seem to show that grain orientations present in this fine-
170 grained layer could have impacted the crystalline orientations of the following layer by playing the role of embryos. Indeed the last layer presents large grains with some **c**-axes oriented along the thermal gradient direction, as observed in the G1 hailstone. The second type of hailstone, G1 (Fig. 6, and Fig. A1 in the Appendix for hailstone F3) also presents several layers but with another arrangement. The large elongated grains are characterized by **c**-axes oriented in the direction of growth. Contrary to the F1 type of hailstone, the microstructure of the core is composed of small grains. From this core, the growth process in
175 the subsequent layer seems to have favored a specific texture with **c**-axes oriented radially along the growth direction. Such a specific texture, that is not favored by growth, can be compared to the one observed in type S1 lake ice (Michel and Ramseier, 1971) that was shown to result from an oriented seed-based growth.

At the end, the French F3 hailstone (see Fig. A1 in the Appendix) is an interesting illustration of the complexity of the layer formation. The core is composed of a limited number of grains, with one main orientation. But this core is surrounded by a
180 large very fine-grained layer. This layer seems to play the role of the core for the subsequent layers that present a S1 type of texture, with radial **c**-axes. In turn, once interrupted in their growth process, the resulting rather large grains give way to a

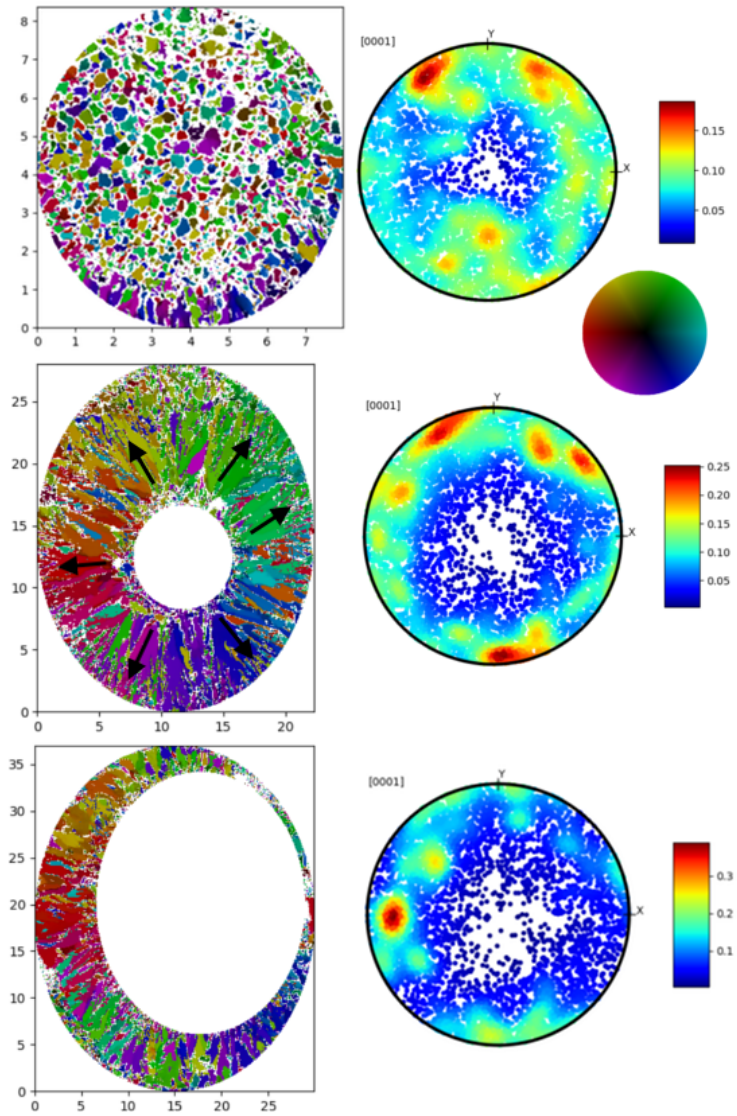


Figure 6. Extracted microstructures of the different observed layers in the German hailstone G1 with the corresponding pole figures. Core layer (top) to external layer (bottom). Black arrows sketch the orientations of a few selected c -axes to help with the analyses. The scale of the orientation color-coded map is in millimeter. The color code is provided by the color wheel.

layer with an S2 type of texture.

Crystal growth during hailstone formation could therefore follow mechanisms similar to those well documented for S1 and S2 lake ices. While S2 ice is characterized by *c*-axes oriented in the plan perpendicular to the growth direction, S1 ice has its *c*-axes preferentially oriented in the direction of growth. Michel and Ramseier (1971) classified these two types of ice based on the departing point of their growth, called the "primary" layer, that acts as seed. The classification provides four types of primary layers, with one resulting into subsequent S1 type of ice owing to a seed-controlled orientation growth, while the three others create S2 type of ice, owing to a growth-controlled orientation mechanism. In order to induce the growth of S1 columnar ice, the primary layer has to form slowly on still water, in such a way that grains, all with vertical *c*-axes, are covering the surface. On the contrary, the primary (seed) layers that lead to S2 ice formation are characterized by randomly oriented small grains, that results either from falling snow, or from an agitated surface. S1 type ice can therefore only grow if grains with *c*-axes oriented in the growth direction are present at the onset of growth, and in conditions still enough to prevent subsequent perturbation of the growth front. Such conditions can not be satisfied in the hailstones similar to F1 since the core is formed of a limited number of crystals with similar orientations. Among all the hailstones studied here (see also Appendix), those with an S2 type texture had cores containing only a few large grains.

Instead, the girdle-type textures observed in the small-grained core of the G1 hailstone provide the necessary seed orientations for a growth of grains with *c*-axes in the radial direction. The large dimension of these radially oriented elongated grains, and the low porosity (transparent ice), must result from relatively undisturbed and slow growth conditions (Knight and Knight, 2005).

Another growth mechanisms was identified by Knight and Knight (1968) as likely to be correlated with the *c*-axis preferred orientations. In this pioneering work, the authors were able to measure *c*-axis orientations by means of etching on the largest crystals from various natural hailstones. Based on the hypothesis that hailstones could result from a spongy growth (with water captured before complete freezing) or not, the authors suggested that spongy hailstones were characterized by large elongated grains with a tangential *c*-axis preferred orientations, while large elongated grains in non spongy hailstones would show more radial *c*-axis orientations. Knight and Knight (1968) concluded that, based on samples from 5 different storms, natural hailstones were likely not resulting from a spongy growth. Thanks to the high resolution of the crystallographic orientation measurements performed here we are able to provide a more accurate picture. Both radial *c*-axes or *c*-axes perpendicular to the growth direction are observed in individual hailstones (e.g. type F1, Fig. 5 and Fig. A3 in the Appendix), and texture is therefore not a clear sign to discriminate a spongy growth, unless considering that various types of growth processes can occur during the formation of these large hailstones.

Hailstones may originate from individual ice crystals created in the clouds. Many studies, well summarized by Furukawa (2015), have shown the relationship between the temperature conditions, the vapor saturation, and the crystallographic orientation of the growth direction for these individual snow crystals (from Nakaya diagram, Nakaya and Marshall (1954)). Snow crystal growth preferentially occurs along the basal crystallographic plan when temperature is above -4°C and between -10 and -22°C , forming the well know dendrite and plate-like structures of snowflakes, while it will preferentially grow along the prismatic plans at temperature between -4 and -10°C , and below -22°C (see figure 25.8 in (Furukawa, 2015)). This classification holds

in a water-saturated vapor atmosphere, and the supersaturation conditions come into play. Whether the cloud conditions met during hailstones formation fall into one of the range of the Nakaya diagram is not clear. In particular, the temperature conditions for hailstones formation estimated by Macklin (1977) seem out of the range of temperatures classically considered for snow crystal formation. Nevertheless, we cannot exclude that the temperature and supersaturation conditions come into play during the still and slow growth phases of the large-grain layers in the hailstones observed. Analyses of crystal orientation of laboratory grown crystals in similar temperature and supersaturation conditions (Fukuta and Takahashi, 1999) could provide additional constraints.

Mechanical behavior of hailstones is of interest for predicting, and preventing, damage caused by hail impact. Hail impact occurs at relatively high strain rate, therefore in the dynamic regime (strain rate above about 10 s^{-1}). In these conditions, as mentioned in part 1, no study exists that takes into account microstructure, texture and porosity as factors influencing the mechanical response. In quasi-static conditions, many studies exist, and we expect a limited effect of grain size on fracture toughness, with variations ranging from about $70 \text{ kPa m}^{1/2}$ for 9 mm grain size to about $90 \text{ kPa m}^{1/2}$ for 2 mm grain size, and no clear effect of texture (see (Schulson and Duval, 2009) for a review). On the contrary, porosity does impact the fracture toughness in quasi-static conditions, with a decrease of about 25% when the porosity increases from 0 to about 15% in volume fraction in fresh granular ice (Smith et al., 1990). In the dynamic loading range (strain rates between 20 and 130 s^{-1}), Georges et al. (2020) showed a strong effect of porosity on the velocity-dependent tensile strength, this latter decreasing by about 25% when the porosity increases from 1 to about 10%. Most of the ice-impact studies performed so far gave little attention to the microstructure and texture of the laboratory grown samples, and resulted into highly dispersed measurements of the strength (see e.g. Shazly et al. (2009); Combescure et al. (2011); Tippmann et al. (2013)). We therefore suggest to pay more attention to grain boundaries and porosities in order to make use of statistical microstructures as close as possible to the hailstone microstructures characterized here. The role to texture on the mechanical strength in dynamic conditions relevant for hail impact remains to be studied. It is only under these conditions that the modeling of hail impact on structures will be efficient (see e.g. Meyers (1994); Erzar and Forquin (2010)).

240 4 Conclusions

This paper presents high resolution characterizations of the microstructure and texture (**c**-axis orientations) of several large hailstones originating from two storms, one that took place in France in 2015, and the other one in Germany in 2013. High spatial and angular resolution observations of textures were made possible by thin section analyses with an Automatic Ice Texture Analyzer. We observed strong microstructure similarities between all hailstones studied, with a quasi-spherical layered structure, in which layers made of small equiaxed grains alternate with layers made of large elongated (columnar) grains. Despite these strong similarities, we recognized two main types of hailstones, each with a specific crystallographic texture within successive layers. One type is mostly made of layers with **c**-axes oriented radially, in the direction of the large grain columns. The other type presents some layers with **c**-axis orientations perpendicular to the radial (and growth) direction. These different types seem to results from the specific properties of the core or the inner contiguous layer (in terms of orientation and

250 number of grains), and are compared to the well-referenced S1 and S2 types of lake ice, providing insight about their formation history.

As so far very few studies exist on the effect of such texture and microstructures on the brittle strength, predictions on their effect on the dynamic response of hailstone ice and resulting damage remains speculative. This study reveals the full microstructure complexity, including layered structure, crystal shapes, orientations and porosity within hailstones that should be taken into
255 account to correctly interpolate laboratory experiments to natural conditions.

5 Data availability

Data are available on Zenodo data base under the reference (Montagnat et al., 2020) (<https://doi.org/10.5281/zenodo.3938956>). Data treatment can be performed by using the freely accessible Python toolbox developed by Thomas Chauve (<https://github.com/ThomasChauve/aita>).

260 Appendix A - Supplementary textures of large hailstones

Figs. A1 and A2 show the microstructure of a French hailstone called F3. This “star geometry” is a typical geometry for wet growth (Knight and Knight, 2005). The sample size was estimated by making the assumption of an ellipsoidal shape. The large axis is about 6.4 cm, the medium axis is about 5.5 cm and the little axis is about 4.5 cm.

The latest French hailstone studied, called F4, is relatively spherical with a diameter of about 3.5 cm (Fig. A3). The sample is
265 opaque which testifies of the presence of a rather homogeneous porosity distributed in the hailstone. Its microstructure and the corresponding pole figure are represented in Figs. A3 and A4.

The German hailstone called G2 is relatively complex, and the different layers are uneasy to distinguish. However, we can observe four different layers including first an ex-centred embryo with relatively large grains, a second layer with relative large grains (about 1 mm diameter), a third layer with small equiaxed grains and a fourth layer with ellipsoidal grains elongated
270 in the direction of growth. The global texture of this hailstone is of girdle-type, with most c-axis orientations in the radial direction.

The last studied hailstone called G3 is a specific one where only two layers could be identified. (Fig. A7) One large layer with homogeneous equiaxed grains and a second small layer with elongated grains. The first layer presents pole figure with a “ring-like” texture, and the second one presents a preferential orientation with two main poles.

275

Author contributions. MM wrote the article and organised the interactions between co-authors. MM made some of the texture measurements and analyses. MB wrote the first draft of the article and made the main measurements and analyses (including microCT). AP participated to

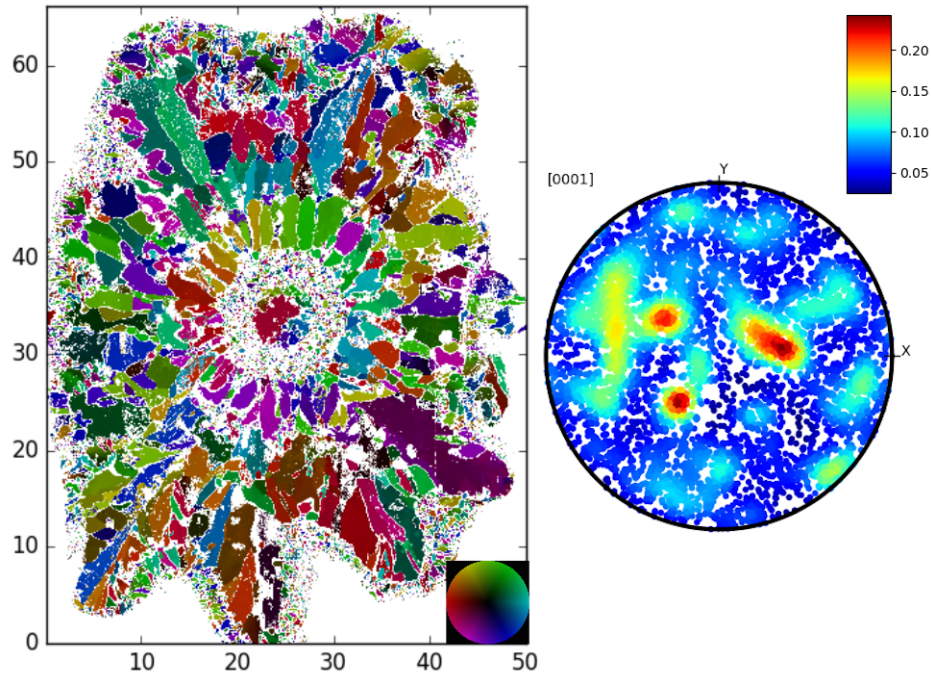


Figure A1. Orientation color-coded microstructure of the French hailstone F3 and the corresponding pole figure (see figure 2 for color-code and scales explanations).

the writing and to the measurements and analyses of the microCT data. PB participated to the writing and analyses of the data. PB and CB provided the German hailstones. PD and PH provided the French hailstones and provided some financial support.

280 *Competing interests.* No competing interests are present

Acknowledgements. Support from CNRS INSIS and INSU institutes is acknowledged. The authors gratefully acknowledge the French Direction Générale de l'Armement (DGA) which supports this research through the framework of project RAPID 142906128. The authors also acknowledge association ANELFA and volunteers who collected the french hailstones in the south west of France. A. Burr is greatly acknowledged for his help during tomography measurements, and T. Chauve for his support on the Python tools he developed. Support from
 285 Labex OSUG@2020 (ANR10Labex56) is acknowledged.

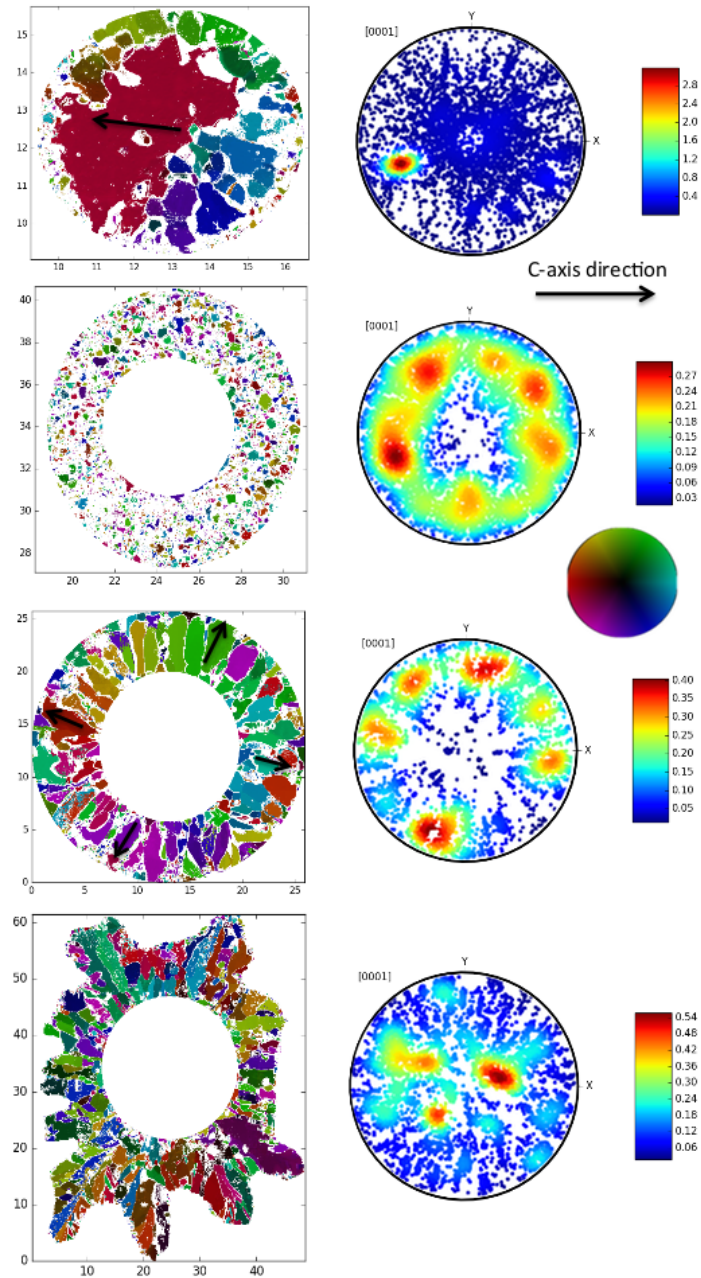


Figure A2. Orientation color-coded representation of the different layers of the French hailstone F3 and corresponding pole figures.

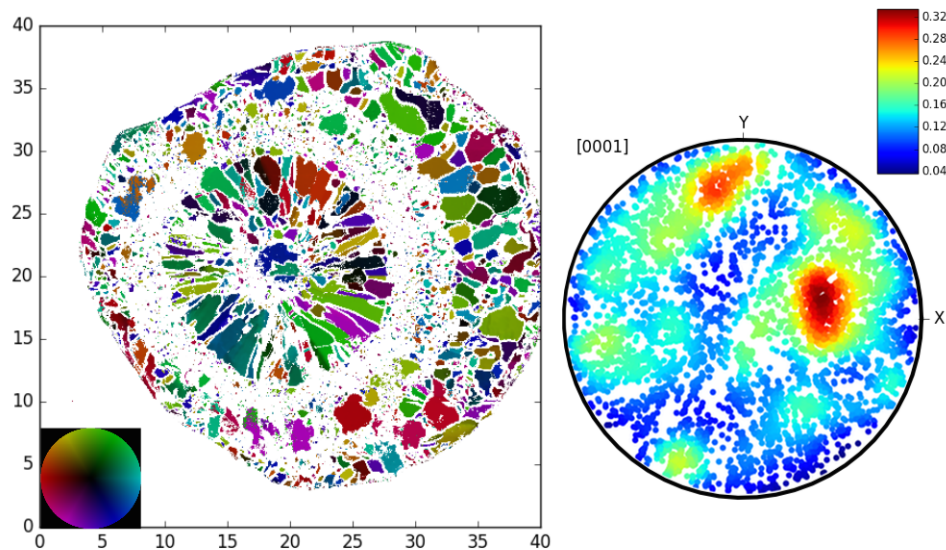


Figure A3. Orientation color-coded microstructure of the French hailstone F4 and the corresponding pole figure.

References

- Anghileri, M., Castelletti, L.-M., Invernizzi, F., and Mascheroni, M.: A survey of numerical models for hail impact analysis using explicit finite element codes, *International Journal of Impact Engineering*, 31, 929–944, 2005.
- Bons, P. D., Elburg, M. A., and Gomez-Rivas, E.: A review of the formation of tectonic veins and their microstructures, *Journal of Structural Geology*, 43, 33–62, 2012.
- Burr, A., Ballot, C., Lhuissier, P., Martinerie, P., Martin, C. L., and Philip, A.: Pore morphology of polar firm around closure revealed by X-ray tomography, *The Cryosphere*, 12, 2481–2500, <https://doi.org/10.5194/tc-12-2481-2018>, <https://www.the-cryosphere.net/12/2481/2018/>, 2018.
- Combesure, A., Chuzel-Marmot, Y., and Fabis, J.: Experimental study of high-velocity impact and fracture of ice, *International Journal of Solids and Structures*, 48, 2779–2790, <https://doi.org/http://dx.doi.org/10.1016/j.ijsolstr.2011.05.028>, <http://www.sciencedirect.com/science/article/pii/S0020768311002198>, 2011.
- Crammer, H.: Eis- und Gletscherstudien, *Neuer Jahrbuch für mineralogie, geologie und paleontologie*, 18, 57–116, 1903.
- Erzar, B. and Forquin, P.: An Experimental Method to Determine the Tensile Strength of Concrete at High Rates of Strain, *Experimental Mechanics*, 50, 941–955, <https://doi.org/10.1007/s11340-009-9284-z>, <https://doi.org/10.1007/s11340-009-9284-z>, 2010.
- Forquin, P. and Erzar, B.: Dynamic fragmentation process in concrete under impact and spalling tests, *International Journal of Fracture*, 163, 193–215, <https://doi.org/10.1007/s10704-009-9419-3>, <https://doi.org/10.1007/s10704-009-9419-3>, 2010.
- Fukuta, N. and Takahashi, T.: The growth of atmospheric ice crystals: A summary of findings in vertical supercooled cloud tunnel studies, *Journal of the atmospheric sciences*, 56, 1963–1979, 1999.
- Furukawa, Y.: Snow and ice crystal growth, *Handbook of Crystal Growth*, pp. 1061–1012, 2015.

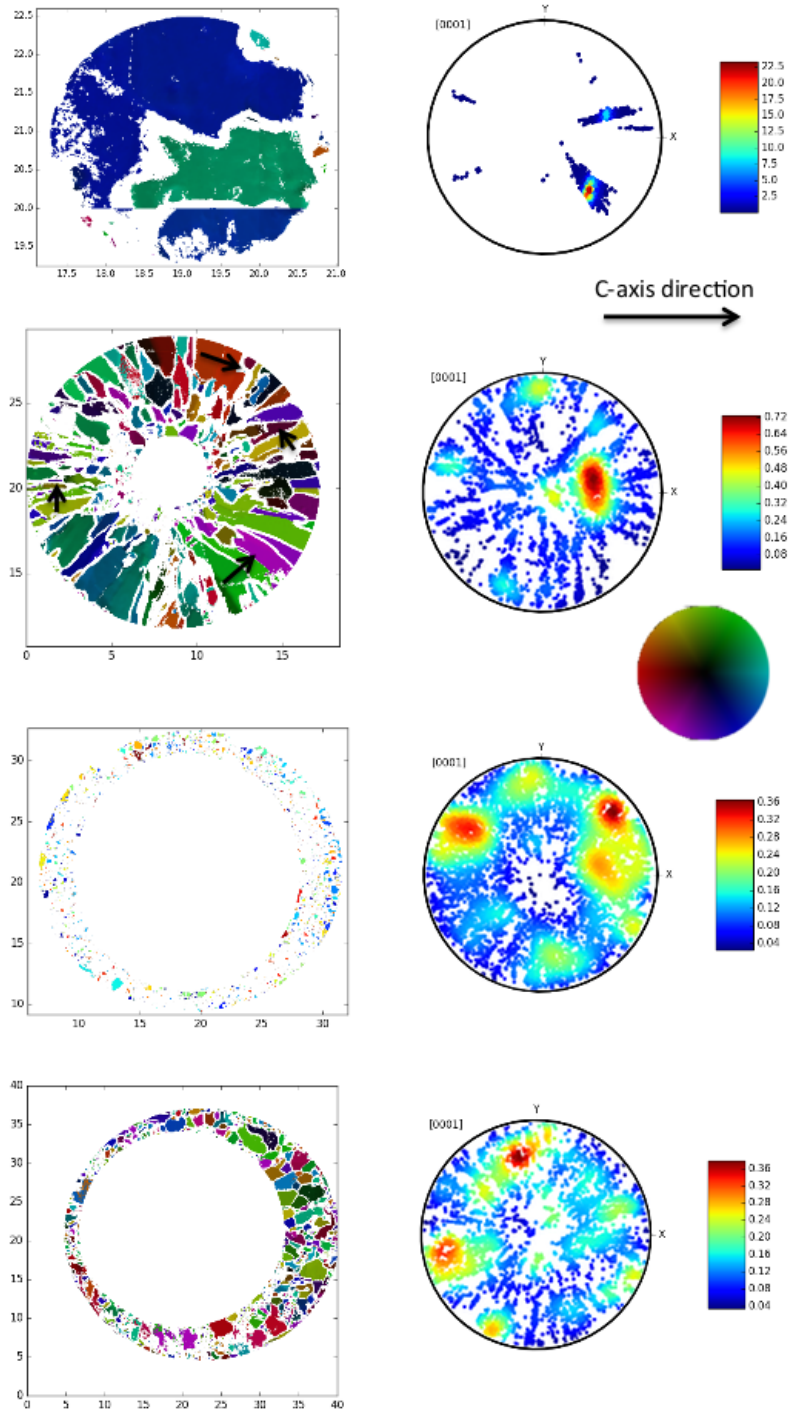


Figure A4. Orientation color-coded representation of the different layers of the French hailstone F4 and corresponding pole figures.

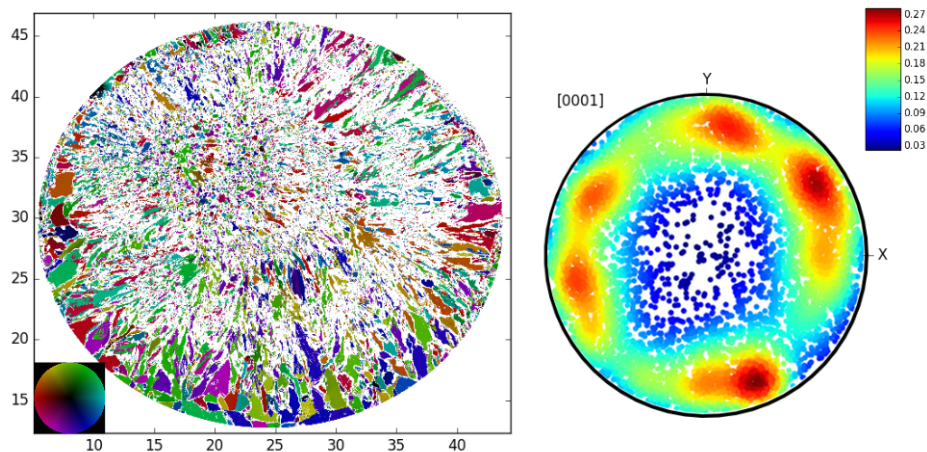


Figure A5. Orientation color-coded microstructure of the German hailstone G2 and pole figure.

- 305 Georges, D., Saletti, D., Forquin, P., and Hagenmuller, P.: Porosity influence on ice dynamic behavior during spalling tests, in prep, 2020.
- Guégan, P., Othman, R., Lebreton, D., Pasco, F., Villedieu, P., Meyssonier, J., and Wintenberger, S.: Experimental investigation of the kinematics of post-impact ice fragments, *International Journal of Impact Engineering*, 38, 786–795, 2011.
- Jouzel, J., Merlivat, L., and Roth, E.: Isotopic study of hail, *Journal of Geophysical Research*, 80, 5015–5030, <https://doi.org/10.1029/JC080i036p05015>, <http://dx.doi.org/10.1029/JC080i036p05015>, 1975.
- 310 Kim, H. and Keune, J. N.: Compressive strength of ice at impact strain rates, *Journal of Materials Science*, 42, 2802–2806, <https://doi.org/10.1007/s10853-006-1376-x>, <http://dx.doi.org/10.1007/s10853-006-1376-x>, 2007.
- Knight, C. A.: Formation of Crystallographic Etch Pits on Ice, and Its Application to the Study of Hailstones, *Journal of Applied Meteorology*, 5, 710–714, [https://doi.org/10.1175/1520-0450\(1966\)005<0710:FOCEPO>2.0.CO;2](https://doi.org/10.1175/1520-0450(1966)005<0710:FOCEPO>2.0.CO;2), [https://doi.org/10.1175/1520-0450\(1966\)005<0710:FOCEPO>2.0.CO;2](https://doi.org/10.1175/1520-0450(1966)005<0710:FOCEPO>2.0.CO;2), 1966.
- 315 Knight, C. A. and Knight, N. C.: Spongy hailstone growth criteria I. Orientation fabrics, *Journal of the Atmospheric Sciences*, 25, 445–452, 1968.
- Knight, C. A. and Knight, N. C.: Very Large Hailstones From Aurora, Nebraska, *Bulletin of the American Meteorological Society*, 86, 1773–1781, <https://doi.org/10.1175/BAMS-86-12-1773>, <http://dx.doi.org/10.1175/BAMS-86-12-1773>, 2005.
- Kunz, M. and Kugel, P. I.: Detection of hail signatures from single-polarization C-band radar reflectivity, *Atmospheric Research*, 153, 565–577, 2015.
- 320 List, R.: New Developments in Hail Research, *Science*, 132, 1091–1098, <http://www.jstor.org/stable/1706746>, 1960.
- Lliboutry, L.: *Traité de Glaciologie - T1 Glace-Neige-Hydrologie Nivale*, Masson et Cie, 1964.
- Macklin, W.: The characteristics of natural hailstones and their interpretation, *Hail: A Review of Hail Science and Hail Suppression*, *Meteor. Monogr*, 38, 65–88, 1977.
- 325 Macklin, W., Merlivat, L., and Stevenson, C.: The analysis of a hailstone, *Quarterly Journal of the Royal Meteorological Society*, 96, 472–486, 1970.

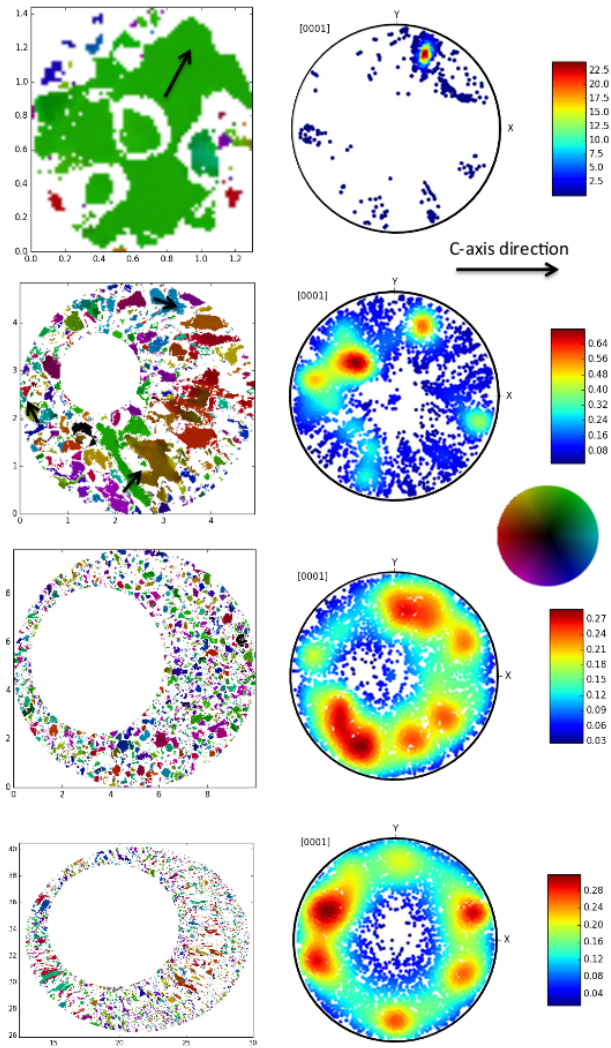


Figure A6. Orientation color-coded representation of the different layers of the German hailstone G2 and corresponding pole figures.

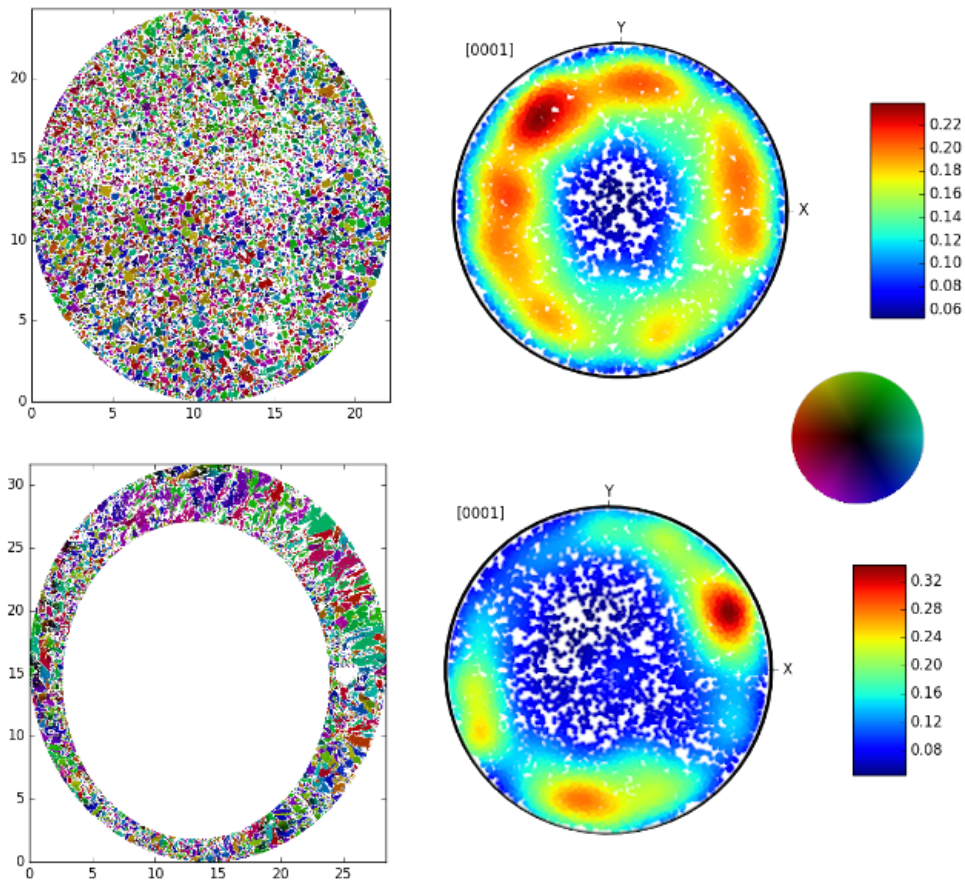


Figure A7. Orientation color-coded representation of the layers of the German hailstone G3 and corresponding pole figures.

- Macklin, W. C., Carras, J. N., and Rye, P. J.: The interpretation of the crystalline and air bubble structures of hailstones, *Quarterly Journal of the Royal Meteorological Society*, 102, 25–44, [https://doi.org/DOI: 10.1002/qj.49710243103](https://doi.org/DOI:10.1002/qj.49710243103), <http://dx.doi.org/10.1002/qj.49710243103>, 1976.
- 330 Meyers, M. A.: *Dynamic Behavior of Materials*, Wiley-Interscience, 1994.
- Michel, B. and Ramseier, R.: Classification of river and lake ice, *Can. Geotech*, 8, 1971.
- Montagnat, M., Weiss, J., Cinquin-Lapierre, B., Labory, P., Moreau, L., Damilano, F., and Lavigne., D.: Waterfall ice: formation, structure and evolution, *Journal of Glaciology*, 56, 225–234, 2010.
- Montagnat, M., Bourcier, M., and Philip, A.: Data: Crystallographic orientations of large hailstones, <https://doi.org/10.5281/zenodo.3938956>,
- 335 <https://doi.org/10.5281/zenodo.3938956>, 2020.
- Nakaya, U. and Marshall, J.: Snow crystals, *American Journal of Physics*, 22, 573–573, 1954.
- Pernas-Sánchez, J., Artero-Guerrero, J., Varas, D., and López-Puente, J.: Analysis of Ice Impact Process at High Velocity, *Experimental Mechanics*, 55, 1669–1679, 2015.

- Peternell, M., Russell-Head, D., and Wilson, C.: A technique for recording polycrystalline structure and orientation during in situ deformation cycles of rock analogues using an automated fabric analyser, *Journal of Microscopy*, 242, 181–188, 2011.
- 340 Puskeiler, M., Kunz, M., and Schmidberger, M.: Hail statistics for Germany derived from single-polarization radar data, *Atmospheric Research*, 178, 459–470, 2016.
- Schulson, E. M. and Duval, P.: *Creep and Fracture of Ice*, Cambridge University Press, <http://dx.doi.org/10.1017/CBO9780511581397>, 2009.
- Schuma, T. E. W.: The theory of hailstone formation, *Quarterly Journal of the Royal Meteorological Society*, 64, 3–21, 345 <https://doi.org/10.1002/qj.49706427303>, <https://doi.org/10.1002/qj.49706427303>, 1938.
- Shazly, M., Prakash, V., and Lerch, B. A.: High strain-rate behavior of ice under uniaxial compression, *International Journal of Solids and Structures*, 46, 1499–1515, <https://doi.org/http://dx.doi.org/10.1016/j.ijsolstr.2008.11.020>, <http://www.sciencedirect.com/science/article/pii/S0020768308004927>, 2009.
- Smith, T., Schulson, M., and Schulson, E.: The fracture toughness of porous ice with and without particles, in: *Proceedings, Ninth International Conference on Offshore Mechanics and Arctic Engineering*, pp. 241–246, 1990.
- 350 Tippmann, J. D., Kim, H., and Rhymer, J. D.: Experimentally validated strain rate dependent material model for spherical ice impact simulation, *International Journal of Impact Engineering*, 57, 43–54, <https://doi.org/http://dx.doi.org/10.1016/j.ijimpeng.2013.01.013>, <http://www.sciencedirect.com/science/article/pii/S0734743X13000201>, 2013.
- Wilson, C., Russell-Head, D., and Sim, H.: The application of an automated fabric analyzer system to the textural evolution of folded ice layers in shear zones, *Ann. Glaciol.*, 37, 7–17, 2003.
- 355